Ensuring a connected structure for Retinal Vessels Deep-Learning Segmentation

Idris Dulau [a]
idris.dulau@labri.fr

Catherine Helmer [b]
catherine.helmer@u-bordeaux.fr

Cecile Delcourt [b]
cecile.delcourt@u-bordeaux.fr

Marie Beurton-Aimar [a]
beurton@labri.fr

[a], France, LaBRI UMR 5800, Bordeaux University
[b], France, INSERM U1219, Bordeaux University

Abstract

Retinal vessels identification plays a critical role in computer-aided diagnosis and analysis of fundus images. While Deep-Learning-based segmentation methods have shown remarkable performances in handling detailed and pathological fundus, they produce disconnected components whereas retinal vessels are a connected structure. In this work, we developed a post-processing pipeline to ensure a connected structure for the retinal vessels networks. The proposed pipeline named VNR for Vessels Network Retrieval, generates segmentations with a single connected component (CC). This is performed by removing artifacts that are pixels-miss-classified as retinal vessels, and by reconnecting branches that are well-classified but disconnected. By retrieving the structural coherence in the retinal vessels networks, we enable measurements such as vessels length, tortuosity and depth of the vessels tree structure in a more reliable manner. We evaluate our results using pixel-wise and structural metrics, comparing against manually labelled groundtruth. Before applying VNR the predicted segmentations had an average Dice score of 0.839 with 174 CCs. As a result, 173 CCs need to be deleted or reconnected. After applying VNR, the segmentations have an average Dice score of 0.840 with only 1 CC. VNR is thus able to retrieve the connected structure of the retinal vessels networks while also keeping or increasing pixel information.

1. Introduction

Retinal vessels segmentation is an essential task in computer-aided diagnosis and in the analysis of fundus images. It involves separating the blood vessels from the background to enable further examination and measurements.

979-8-3503-3337-4/23/$31.00 ©2023 IEEE

In the last decade, Deep-Learning segmentation outperformed other methods and produces very good results for this task [9, 3]. Especially, it handles detailed, contrasted and pathological fundus images. However, the Deep-Learning segmentation process results in many disconnected components, including branches of the retinal vessels tree and artifacts [6]. These artifacts are miss-classified components that should be considered as background rather than retinal vessels. The branches should be reconnected to form a connected tree-like structure. In this work, we developed a method to address the post-processing of those Deep-Learning segmentations by ensuring a connected structure for the retinal vessels networks. Our approach aims to improve the consistency and the coherence of the retinal vessels structure, enabling reliable measurements such as vessels length, tortuosity and depth of the vessels tree structure. In Section 2, we surveyed state-of-the-art post-processing techniques for artifacts removal and for retinal vessels reconnection . Additionally, we presented Deep-Learning approaches for preserving structural integrity , including network designs, loss functions, and evaluation metrics. The purpose of this analysis is to establish various baselines for the application of our proposed pipeline named VNR for Vessels Network Retrieval. In section 3, we gave technical explanations and illustrations about the steps that compose VNR, which takes Deep-Learning predicted segmentations as input and generates segmentations with a single connected component (CC). In Section 4, we performed experiments to evaluate the proposed VNR. To ensure reproducibility, we utilized publicly available datasets to compare our results against manually labeled groundtruth and state-of-the-art techniques. Additionally, we detailed our data preparation process and the evaluation metrics we used, including pixel-wise and structural metrics. In Section 5, we provided a thorough analysis of our obtained results to evaluate the strengths and limitations of VNR. We justified our algorithmic decisions based

on the characteristics of the retinal vascular structure and its inherent constraints. In Section 6, we drew upon our findings to provide a meaningful conclusion and outline potential directions for future research in the field.

2. Related Work

2.1. Segmentation post-processing

Artifacts removal There is a scarcity of research papers dedicated to artifact removal in the field. Typically, this aspect is included towards the conclusion of network architecture papers. As depicted in [6], the existing post-processing techniques applied to retinal vessels segmentations can be classified into three categories: Morphological operations, Threshold and Deep-Learning Network-Followed-Network. The techniques that rely on morphological operations use erosion & opening [20], or skeleton [21] [22]. Threshold techniques are more diverse whether on the feature maps [7], on the connected components' elongatedness [14], or on the connected components' areas, either by an absolute threshold [25] [8] or a relative threshold [6]. Finally, we will disregard the Deep-Learning post-processing techniques such as [24] due to their probabilistic nature and thus incapability to ensure an exact behaviour.

Vessels reconnection Retinal vessels reconnection techniques could be classified in two categories, the ones that ensure a connected structure and the others. Moreover, some techniques presents how to extend the thickness during the reconstruction process, while other concentrates solely on the skeleton. For those that ensure a connected structure: in [12], the segmentation is skeletonized then each endpoint is connected to another endpoint using the shortest path if satisfying a specific angle condition. It stops when there is no possibility to create any more path and keeps the biggest CC. In [11], there is a distinction between the biggest CC and the smaller CCs. Each smaller CC is reconnected to the biggest CC by fitting a polynomial curve to the nearest points of the biggest CC in the smaller CC. Reconnection is not necessarily performed from the endpoint of the smaller CC. Nothing is removed during the process, which means nothing is regarded as an artifact. Now, for the post-processing techniques that does not ensure a connected structure: in [8], the segmentation is skeletonized and there is a separation between the biggest CC and the smaller CCs. Each smaller CC endpoint is connected to the biggest CC using the shortest path if satisfying a specific tortuosity and path intensity condition. The technique has been developed before the rise of Deep-Learning but the path intensity could correspond to the probability map generated by a Deep-Learning segmentation. Also, no artifacts are deleted. In [1], the segmentation is skeletonized then a maximal reconnection distance is chosen and circles are generated centered on endpoints with diameter being the maximal reconnection distance. The image is again skeletonized to produce a reconnection between endpoints for overlapping circles. Still no removal during the process. Finally, in [5], the biggest CC and the smaller CCs are distinguished in the skeletonized segmentations. Each biggest CC crosspoint is reconnected to each smaller CC endpoint by fitting a polynomial curve using the shortest distance if satisfying a specific tortuosity and path length condition.

2.2. Deep-Learning for structural preservation

Additionally, we explored Deep-Learning approaches for preserving structural integrity, including network designs, loss functions, and evaluation metrics. The purpose of this analysis is to establish various baselines for the application of our methods. The main state-of-the-art Deep-Learning methods for topology-preservation of curvilinear structures including retinal vessels are DVAE [2], clDICE [17] and JFTN [4]. Those three methods are willing to improve the connectivity/topology/structure coherence and evaluate it in their results. DVAE [2] is a Network-Followed-Network that uses a U-Net [16] to generate intermediate segmentations and their Denoising Variational Auto-Encoder with a class-weighted Binary Cross Entropy loss function to produce the final segmentations. To evaluate the topological coherence of the outputs 1000 connected path per test image are randomly chosen from the groundtruth and are compared to the corresponding path in the segmentation. The prediction is considered correct if the length difference is within 10%. Otherwise, it is labeled as incorrect. If the path does not exist, the prediction is classified as infeasible. clDICE [17] proposes a Deep-Learning architecture with a new pixel-wise loss function that weights the Dice loss [10] with a new centerline Dice loss based on the skeletonized version of the segmentation. The Mean Absolute Error on the Betti numbers (Number of foreground CC and number of background CC) is used to asses the structural coherence. The method has been experimented using U-Net and shown better scores for topological and pixel-wise evaluations. JFTN [4] is a new architecture that mixes U-Net and VGG-16 [18], adds a custom Gated Attention Unit module (GAU) and a custom Feature Interactive Module (FIM). The network combines pixel information and boundary information in the FIM and uses Binary Cross Entropy as a loss function. The evaluation is done using Completeness, Correctness and Quality that are described in [23] as equivalent to recall, precision and Jaccard and thus are not giving structural coherence information.

3. Methodology

The primary objective of the proposed pipeline named VNR is to enable measurements of the predicted segmentations. To do so, a connected structure segmentation is

required, as it is the anatomical arrangement of the vessels. Without a connected structure, several measurements (*e.g.* vessels length, tree depth, vessels tortuosity) cannot be accurately determined. As denoted in [6], without post-processing, the only part that can be measured is the biggest connected component in the segmentation (denoted as $CC = 1$). However, such segmentation yields a reduced amount of information compared to the originally predicted segmentation (denoted as $Pred$). To face out the current limits of $Pred$, we proposed a pipeline composed of two methods, and that ensures a connected vessels structure.

3.1. Gap Filling procedure

The first method we proposed to overcome the limitations of $Pred$ is the gap filling method. It is motivated by an analysis of the CC in $Pred$ for the images in each dataset. As also expressed in [6], in the CC's area distribution sorted by decreasing order, it exists a threshold: Best THLD (see Fig. 1), where everything above is vessels that should be reconnected. What is under are artifacts and smaller vessels.

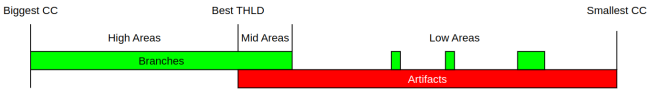

Figure 1. CCs area distribution

The method efficiently retains big vessels that require reconnection, but it also eliminates smaller vessels in the process. In order to also keep vessels under the threshold, we proposed another gap filling procedure. The idea is to aggregate CCs together, according to several criteria, in order to produce bigger vessels that can be distinguished from artifacts. The algorithm can be expressed as follows:

Finding candidates This initial stage involves skeletonizing the vessels, extracting the endpoints (*i.e.* white pixels that have only one white neighbor), extracting the crosspoints (*i.e.* white pixels that have three or more white neighbors) and determining the mutual closest pairs of endpoints-endpoints and endpoints-crosspoints. The distance is calculated using the Euclidean metric. Candidates are thus the pairs of mutual closest points as illustrated in Fig. 2 Additionally, to enhance computational efficiency, we remove the CCs whose areas are under 5 pixels before extracting the endpoints. Whatever, these CCs are unlikely to be reconnected based on the subsequent candidate filtering step.

Filtering candidates Once the initial candidate pairs have been obtained, the next step involves filtering these candidates based on various conditions. Firstly, we verify whether the elements of the pair belong to the same CC. If they do, we discard the pair as the elements are already connected. Next, we determine the smallest CC between

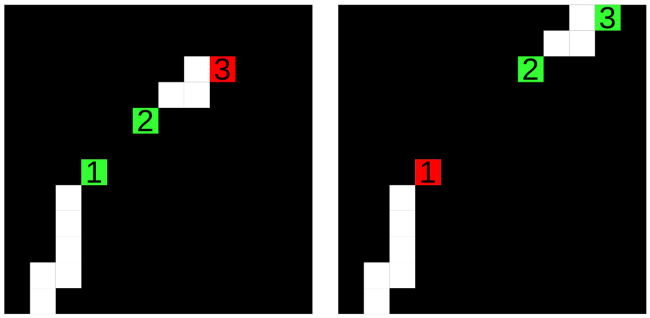

Figure 2. Illustration of a predicted segmentation at pixel-level, where 1-2 is the closest pair (left) and 2-3 is the closest pair (right).

the CCs of the two candidates. Within this smallest CC, we extract the nearest endpoint or crosspoint to the candidate. Subsequently, we calculate the angle formed by these three points at the candidate within the smallest CC. We keep the pair if the angle deviates at maximum 45 degrees from a straight line. Furthermore, we employ the Bresenham's line algorithm to extract pixel values along a line between the candidate pair. This enables us to detect the presence of an existing vessel in the path. In such case, we don't reconnect.

Reconnecting vessels At this stage of the process, the candidate pairs that fulfill all the aforementioned conditions are selected for reconnection. Unlike alternative approaches that utilize splines of second or third order, our reconnection path is established as a straight line. The rationale behind this choice will be thoroughly explored and discussed in the subsequent section dedicated to the discussion (Section 5).

Propagating thickness In order to effectively propagate the thickness along the previously drawn line path, several key steps are undertaken. Firstly, a neighboring kernel (5x5) is extracted around the endpoint of the smallest CC within the candidate pair. This kernel serves as a reference for the desired thickness. Next, the extracted kernel is replicated over the black pixels at each element of the drawn line. This process ensures that the thickness is maintained consistently along the vessel path. The rationale behind this approach is rooted in several observations. Firstly, vessels typically exhibit a uniform thickness over short distances. Additionally, there tends to be a change in the vessels thickness around crosspoints. By selecting the thickness of the smallest CC, we ensure that the reconnection of two vessels is performed with the appropriate and coherent thickness. Upon completing the four aforementioned steps of the Gap filling procedure, results can be illustrated as in Fig. 3. At the left, the predicted segmentation with gaps to fill. In the middle, the post-processed segmentation where the reconnection paths between gaps that could be filled are drawn in green. At the right, the manually labeled groundtruth.

Figure 3. Zoomed images of the Gap Filling procedure: predicted segmentation (left), post-processed segmentation (mid) where filled gaps are drawn green, manually labeled groundtruth (right).

3.2. Rebranch or Remove procedure

In the preceding Gap Filling procedure (Section 3.1), the emphasis was solely on reconnection rather than deletion, with only minimal removal of small artifacts. In cases where the conditions for reconnection were not met, paths were not established, but the vessels themselves remained intact without any deletion. However, in this subsequent procedure, the approach shifts to not only attempting vessels reconnection but actively removing elements that fail to meet the specified conditions. This approach enhances the overall quality and reliability of the vessels segmentations by ensuring a connected vessels structure.

Finding candidates To identify candidates for reconnection, we first distinguishes between the biggest CC and all the smaller CCs. For each smaller CC, we extract all of its endpoints. Then, for each endpoint, we locate its nearest endpoint or crosspoint within the same CC. Subsequently, we obtain the pixels along a line connecting the nearest endpoint or crosspoint to the original endpoint. Finally, if there exists a main point (point within the biggest CC) along this line, we consider the endpoint and its nearest main point as a candidate pair. Otherwise, the smaller CC is removed.

Filtering candidates After the pairs extraction, the only filtering requirement is that the length of the reconnection path has to be smaller than the length of the smaller CC. If multiple endpoints from the same CC are candidates for reconnection, only the first endpoint matching the conditions is reconnected, removing others candidates from the queue.

Figure 4. Zoomed images of the Rebranch or Remove procedure: predicted segmentation (left), post-processed segmentation (mid) with the added reconnection paths (green) and the removed elements (violet), manually labeled groundtruth (right).

Next steps of reconnecting vessels and propagating thickness are the same as for the Gap Filling procedure (Section 3.1). Results can be illustrated as in Fig. 4. At the left, the predicted segmentation. In the middle, the post-processed segmentation where the reconnecting paths are drawn in green and the removed elements in violet. At the right, the manually labeled groundtruth.

Some may have noticed in the figure that the violet elements should not be removed according to the groundtruth. These limitations will be discussed afterwards (Section 5).

4. Results

4.1. Retinal Vessels Datasets

To assess VNR's generalizability, and for enabling future enhancements of this work, we evaluated performances on four public datasets: *DRIVE* [19], *DUALMODAL2019* [26], *HRF* [13] and *LESAV* [15]. Collectively, the four datasets comprise 137 fundus images with associated binary manual annotations of retinal vessels. Images of the four datasets, illustrated in Fig. 5, show the diversity of the fundus images and their vessels networks. These images have been captured using different materials (*e.g*. Canon CR5 non-mydriatic with 3CCD sensor, OT-110M, Hefei Orbis Biotech LTD, ...), from different angles (*e.g*. optic disk centered, macula centered, ...), with different resolutions (*e.g*. 565*584, 3504*2336, ...) and comprise various pathological signs (*e.g*. exudates, glaucoma, ...).

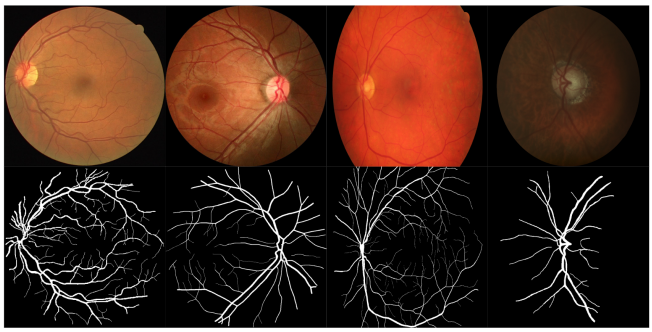

Figure 5. DRIVE, DUALMODAL2019, HRF, LESAV

4.2. Predicted Segmentations

In order to obtain the predicted segmentations required for VNR input, we performed an independent Supervised-Learning training for each of the four datasets using the aforementioned segmentation techniques that we referred as UNetBN [6] and clDICE [17] (Section 2.2). The clDICE method should maximize the structural coherence of the predicted segmentations whereas the other method maximizes the pixel-wise quality. The DVAE [2] and JFTN [4] methods are not used as discussed afterwards (Section 5).

4.3. Evaluation Metric

The goal of VNR is to provide a fully connected vessels structure, thus we evaluate the number of CC in the post-processed segmentations as suggested in [6]. It is crucial to note that accurate measurements of the retinal vessels can only be fully extracted when there is a single CC within the segmentations. To prevent a good ranking of connected segmentations with low Precision or low Recall, we incorporated a pixel-wise information with the Dice metric.

- Precision = $\frac{TP}{TP+FP}$
- Recall = $\frac{TP}{TP+FN}$
- Dice = $\frac{2*TP}{2*TP+FP+FN}$

4.4. Experiments

Results of our experiments are shown in Tables 1 & 2. The VNR method is applied using the predicted segmentations ($Pred$) of clDICE (Table. 1) and UNetBN (Table. 2) over the four aforementioned datasets. The tables show, for each dataset and on average, the Dice score and number of CCs for the $Pred$, for their measurable parts $CC = 1$ (*i.e.* bigger connected part) and for the VNR application over $Pred$. The tables also give information about the gain of using VNR instead of using $CC = 1$ and instead of using $Pred$. For both $Pred$ from clDICE and UNetBN, the VNR method fulfills its goals by ensuring a fully connected structure with in average no loss in the Dice score or a slight gain. An average similar Dice score between $Pred$ and VNR is justified by the unwanted removal of some disconnected vessels that is balanced by other added reconnection paths with appropriate thickness. Results show in average a removal of 173 CC for the $Pred$ of clDICE (Table. 1) and 113 CC for those of UNetBN (Table. 2) . This thus demonstrated that VNR is robust to the differences in the structural coherence of $Pred$. Results of VNR are illustrated in Fig. 6 showcasing differences between the predicted segmentation (CC=77) and the segmentation after applying VNR (CC=1).

Datasets	Metrics	$Pred$	$CC = 1$	VNR	Gain over $CC = 1$	Gain over $Pred$
DRIVE	Dice	0.823	0.821	0.825	+0.004	+0.002
	CC	212	1	1	-	-211
DUALMODAL2019	Dice	0.841	0.829	0.840	+0.011	-0.001
	CC	225	1	1	-	-224
HRF	Dice	0.830	0.821	0.828	+0.007	-0.002
	CC	151	1	1	-	-150
LESAV	Dice	0.863	0.855	0.866	+0.011	+0.003
	CC	109	1	1	-	-108
Average	Dice	0.839	0.831	0.840	≈ 0.009	≈ 0
	CC	174	1	1	-	-173

Table 1. Evaluations and comparisons of the VNR pipeline applied over segmentations predicted by the clDICE method ($Pred$). Results are compared in term of Dice and number of CCs. $CC = 1$ is the measurable part of $Pred$, *i.e.* it's bigger connected part.

Datasets	Metrics	$Pred$	$CC = 1$	VNR	Gain over $CC = 1$	Gain over $Pred$
DRIVE	Dice	0.832	0.833	0.834	+0.001	+0.002
	CC	122	1	1	-	-121
DUALMODAL2019	Dice	0.848	0.822	0.847	+0.025	-0.001
	CC	121	1	1	-	-120
HRF	Dice	0.833	0.826	0.831	+0.005	-0.002
	CC	150	1	1	-	-149
LESAV	Dice	0.864	0.861	0.867	+0.006	+0.003
	CC	65	1	1	-	-64
Average	Dice	0.844	0.835	0.845	≈ 0.010	≈ 0
	CC	114	1	1	-	-113

Table 2. Evaluations and comparisons of the VNR pipeline applied over segmentations predicted by the UNetBN method ($Pred$). Results are compared in term of Dice and number of CCs. $CC = 1$ is the measurable part of $Pred$, *i.e.* it's bigger connected part.

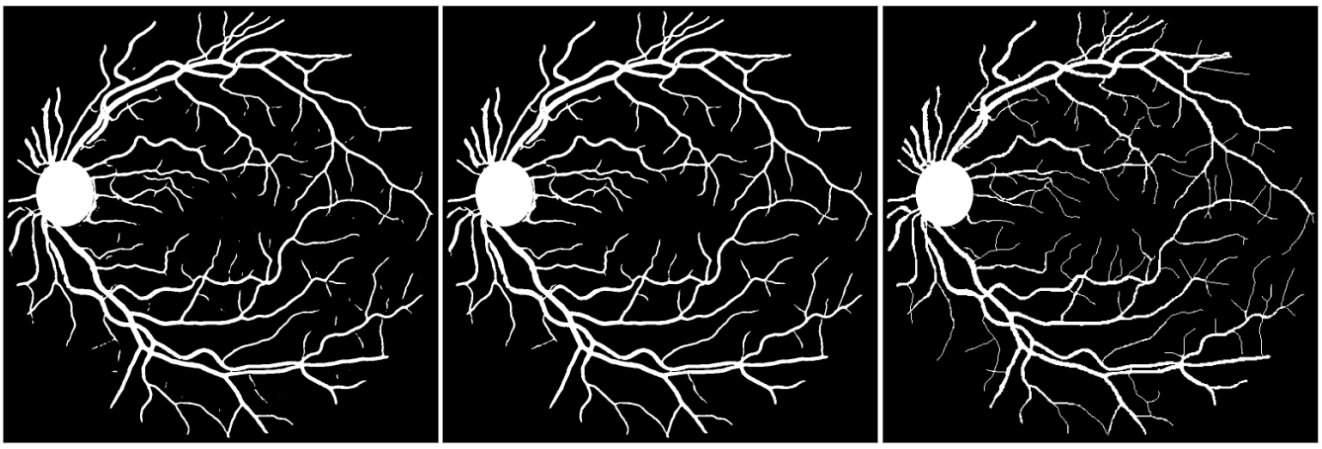

Figure 6. Predicted segmentation Dice=0.847 CC=77 (left), segmentation after applying VNR Dice=0.848 CC=1 (mid), groundtruth (right)

5. Discussion

Vessels Network Retrieval Results of the VNR method are shown in term of Dice and number of CCs in Tables 1 & 2. The experiments show that VNR is able to retrieve the connected structure of the retinal vessels networks while also keeping or increasing pixel information. The superiority of VNR compared to $Pred$ is readily apparent when considering the number of CCs, but it may not be as apparent when comparing it to $CC = 1$ since both methods produce a connected structure. Besides the dice gain, the advantages of VNR over $CC = 1$ are in term of retrieved branches and reconnection paths. This behaviour thus enables measurements such as vessels length, tortuosity and depth of the vessels tree structure in a more reliable manner. One potential counterargument to the necessity of post-processing techniques like VNR is the idea that if predicted segmentations were fully connected, such post-processing steps would be rendered unnecessary. The argument posits that by optimizing Deep-Learning algorithms to produce segmentations with complete connectivity, the need for additional processing would be eliminated. However, it is important to consider the probabilistic nature of Deep-Learning segmentations. Due to this inherent uncertainty, it is impossible to ensure a complete connectivity in every prediction. While deterministic algorithms could generate connected segmentations, they cannot handle the complex and nuanced features present in detailed, contrasted, and pathological fundus images. Moreover, methods that aim to preserve structural coherence, such as clDICE still do not guarantee fully connected segmentations. In comparison, segmentations generated by UNetBN, which primarily focuses on pixel-wise quality, exhibit a lower average number of CC with 114 CC, compared to clDICE-based segmentations with 174 CC. Moreover, relying on the goal of achieving fully connected segmentations in one process overlooks the other challenges posed by intricate fundus image characteristics. It is already very difficult to guaranty for any fundus, a high-quality segmentation taking only into account the pixel-wise quality. Therefore, VNR is necessary to provide further removal and reconnection steps for the purpose of enabling reliable measurements of the retinal vessels segmentations. Furthermore, we previously discussed the DVAE method, although it was not utilized in our experiments. This decision was made because while DVAE effectively reduced the number of CCs with an average of 39 CC, it also resulted in significantly wider vessels thickness. The widening of vessels is a consequence of the second network in the architecture which expands all the vessels, ultimately leading to a higher degree of connectivity among the elements. It is important to note that this behavior is fundamentally incompatible with accurate measurements, thus we opted not to employ the DVAE method.

State-of-the-art techniques Before determining the final combination of steps for VNR (Section 3), we thoroughly explored various alternative approaches. Among these alternatives, we considered two state-of-the-art techniques, which are designed to ensure a connected structure within the vessels networks. Initially, we examined the method proposed by Mou *et al*. [11]. This method involves reconnecting the closest branch points to their closest main point (point within the biggest CC, as a reminder). However, we observed that this approach can lead to the reconnection of branches from non-endpoints or non-crosspoints, which compromises anatomical coherence. We also investigated the work of Niemeijer *et al*. [12] which involves the reconnection of endpoints to endpoints. However, the groundtruth indicates that the correct reconnection points are mostly located on plain structures of the main vessels in the network, rather than at endpoints or crosspoints. Consequently, the method resulted in either very few reconnections or lengthy and incorrect reconnection paths. Consequently, we did not incorporate these methods in VNR.

Gap Filling procedure Before implementing the current Gap Filling procedure in VNR, we explored an alternative approach based on the method proposed in [6]. This method aimed to remove all artifacts while keeping the most possible amount of branches. However, the amount of kept branches can be very low if the method's threshold is not well selected. While it was possible to reconnect the remaining branches using the Rebranch or Remove procedure of VNR, this approach resulted in a significant loss of information. To mitigate the information loss and preserve a more comprehensive representation of the retinal vessels networks, we introduced the current Gap Filling procedure in VNR. This new procedure effectively fills the gaps in the vessels networks while minimizing the loss of important vessels information. As mentioned in 3.1 by aggregating small CC (under conditions) with the Gap filling procedure, we make them big enough to be considered branches and not artifacts anymore. Also instead of in [1] where reconnection distance is manually chosen, we found very relevant to use the skeletonized branch length as a condition to avoid very long or very short reconnection distances that could not fit all specific branch size. In determining the conditions for the procedure, we opted to select candidates based on the mutual shortest pair and subsequently discard those belonging to the same CC. While an alternative approach could involve checking pairs that do not belong to the same CC, this would result in significantly longer reconnection paths. Our objective was to ensure that the reconnection path remained smaller than the length of the CC. Therefore, by employing our chosen approach, we avoided the need to verify the path length while achieving the desired outcomes. In predicted segmentations, some part of vessels can be very small and very far from the others as in Fig. 4. The violet elements, according to the groundtruth, should not be removed. However, it is impossible to determine whether these elements are small parts of vessels. Even if we assumed the hypothesis that the violet elements represented vessels requiring reconnection, it remains challenging to determine whether they should be reconnected to the topmost branch or the bottommost branch. Furthermore, even with this knowledge, we encounter a significant obstacle due to the small size of the violet CC and the disproportionately long reconnection path in relation to the CC itself. Such limitations prevent us from accurately determining how to reconnect the violet CC, potentially resulting in an incorrect continuation of the branch. Consequently, these factors can lead to false measurements and compromise the coherence of the results. In those situations, the gap filling procedure may not capture all the small vessels; however, it still outperforms the method proposed in [6] in this regard. Additionally, in rare instances, the procedure may result in incorrect connections of the endpoints of the outermost vessels when they are at the same time disconnected and identified as mutual closest pairs. Nonetheless, this issue could be mitigated in future research by incorporating artery and vein information.

Remove or Rebranch procedure After applying the Gap Filling procedure of VNR, the remaining artifacts have to be removed, and the branches have to be reconnected. In addition to the existing conditions in the Remove or Rebranch procedure, we investigated on various angles conditions and analyse if we could extract some generic patterns. Finally, the angle of reconnection is disregarded since vessels can be reconnected in any angles. Also, based on the findings we mentioned discussing the state-of-the-art techniques, we found out that the correct reconnection points are primarily located on plain structure (*i.e*. points with only two neighbors when the structure is skeletonized) of the main vessels of the networks, and not at main endpoints or crosspoints. Thus for this Remove or Rebranch procedure we chose to reconnect the closest branch endpoints to the closest main point. There are further inquiries that can be made regarding the methods used to establish the reconnection paths, specifically through splines or straight lines. The splines technique relies on the selection of the control points and the endpoint. If the endpoint is not provided and spline interpolation is employed to determine it, the behavior of the reconnection path can significantly differ even with a slight variation of a single pixel in the control points, leading to highly distorted and false reconnection paths. When the endpoint is given, two scenarios arise. In the case of a lengthy path, the splines approach remains highly influenced by the control points, resulting in abrupt angles at certain points and potential distortions. On the other hand, for shorter paths, the behavior tends to be less anatomically inaccurate, resembling a nearly straight line, yet still prone to distortions. In contrast, straight lines do not require close monitoring. To summarize, for small reconnection paths, straight lines prove to be more effective. However, when a long reconnection path is necessary, it suggests a possible deficiency in the quality of the predicted segmentations.

Choroidal vessels & Line shaped pathologies Choroidal vessels refer to the blood vessels that are part of the choroid, which is a layer of tissue located between the outermost layer of the eye (sclera) and the innermost layer (retina). The choroid contains a dense network of blood vessels, while line-shaped pathologies can resemble to vessels. These similarities pose a challenge for Deep-Learning algorithms, as they may mistakenly classify them as retinal vessels. We investigated on methods to differentiate them from the retinal vessels. Initially, we considered a criterion that their nearest endpoint to the main structure might not necessarily be the closest to the optic disk. However, we discovered instances where this criterion also applied to retinal vessels. Similarly, we thought that if the distances between

their endpoints and the optic disk were too close, indicating nearly perpendicular alignment with the main structure, they would not be classified as retinal vessels. However, we encountered cases where retinal vessels exhibited this characteristic as well. Ultimately, when segmented, these structures can possess identical descriptions to retinal vessels, including similar shapes, positions, tortuosity, and neighboring distances. Consequently, the most effective approach to mitigating their inclusion is through enhancing the predicted segmentations, as there is currently no discernible evidence to differentiate them at post-processing stage.

Inner branches reconnections Lastly, we delve into the details of another of our investigated methods called Inner branches reconnections. The goal of the method is to locally reconnect vessels that are already globally connected. As an example, in Fig. 7, the white pixels are globally connected (CC=1 in the full vessels networks) but in this zoomed part, the green pair 1-2 can be locally connected. First, we find the mutual closest pairs of endpoints. Then for each pair we define a rectangle whose diagonal is the euclidean path between the endpoints pair. We keep the pairs that belong to a different CC in their rectangle, meaning that there is no path between them in the rectangle. Then for each endpoint of the pair, we find its nearest crosspoint. We then use the two crosspoint-endpoint informations to determine the direction from crosspoint to endpoint. From there we want to reconnect endpoints pair solely under three criteria. First, the crosspoint to endpoint directions have to be opposite. Second, the leftmost endpoint should reconnect rightwards, the rightmost endpoint should reconnect leftwards, the topmost endpoint should reconnect downwards, and the bottommost endpoint should reconnect upwards. Third, the reconnection path to be created have to be free of any existing vessels. This algorithm is depicted in Fig. 7. As illustrated, both yellow and cyan path are anatomically coherent. This shows a limit to this algorithm but also to general retinal vessels segmentation post-processing techniques: it is impossible to predict the reconnection path taken by a vessel. Thus, we did not add this further step to the pipeline as we already ensured a connected structure with current VNR.

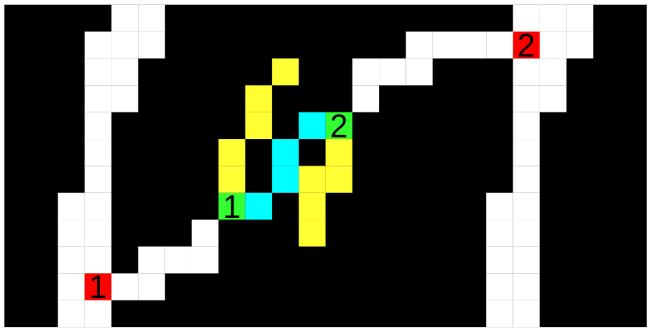

Figure 7. Illustration of the inner branches reconnection at pixel level. 1-2 is a closest pair of endpoints (green). 1-1 and 2-2 are endpoint-crosspoint (red) pairs. The pair of 1 goes top/right and the pair of 2 goes bot/left. The endpoint 1 is positioned at bot/left of the endpoint 2. There are no vessels between endpoints pair 1-2. Yellow and cyan paths are anatomically coherent vessels patterns.

6. CONCLUSION

In this study we proposed a post-processing technique named VNR for Vessels Network Retrieval. VNR ensures a connected structure for retinal vessels Deep-Learning segmentation. VNR enables measurements such as vessels length, vessels tortuosity and depth of the vessels tree structure in a reliable manner. VNR has been tested over segmentations that maximizes pixel-wise quality and other that preserve structural coherence. The experiments has been performed over four public datasets and performances were evaluated with a pixel-wise metric, the dice score and a structural metric, the number of CC. Before applying VNR the predicted segmentations had an average Dice score of 0.839 with 174 CC. After applying VNR, the segmentations have an average Dice score of 0.840 with only 1 CC. The huge CCs reduction is not correlated to a huge dice increase because reconnection paths are mostly made of few pixels. However, such small paths enable to measure previously disconnected branches. VNR is thus able to retrieve the connected structure of the retinal vessels networks while also keeping or increasing pixel information. VNR outperforms all the state-of-the-art methods for the purpose of ensuring a connected structure. However, even with our analysis of the general patterns, there is nothing for us and for others that could assert that every reconnection path is well placed. And it is also the case for the vessels in the predicted segmentations. This is inherent to the individuality of the vessels structures. We know that vessels are connected in a tree-like manner, but besides that, the path taken by the vessels, their length, their thickness and everything that is measurable is unpredictable for a specific case. This is the reason under the need for measurements, specific patterns can inform about patients status, but this is also what justifies the impossibility to assert the correctness of the generated reconnection paths. In light of these considerations, there are two potential avenues to explore. Either relying on mean measurements can be deemed sufficient for diagnosis, acknowledging the limitations and challenges associated with the structural, generalizability and classification problems inherent in segmentation-based approaches. Alternatively, it becomes imperative to explore others diagnostic strategies that directly analyze the fundus images, aiming to bypass the need for segmentation steps and overcome the aforementioned drawbacks. By pursuing the latter approach, a direct diagnosis can be derived from the fundus images, potentially offering a solution that mitigates the inherent limitations in segmentation-based methodologies and enhances the overall exactness of the diagnostic process.

References

[1] Aws A Abdulsahib, Moamin A Mahmoud, Hazleen Aris, Saraswathy Shamini Gunasekaran, and Mazin Abed Mohammed. An automated image segmentation and useful feature extraction algorithm for retinal blood vessels in fundus images. *Electronics*, 11(9):1295, 2022.

[2] Ricardo J Araújo, Jaime S Cardoso, and Hélder P Oliveira. A deep learning design for improving topology coherence in blood vessel segmentation. In *Medical Image Computing and Computer Assisted Intervention–MICCAI 2019: 22nd International Conference, Shenzhen, China, October 13–17, 2019, Proceedings, Part I 22*, pages 93–101. Springer, 2019.

[3] Chunhui Chen, Joon Huang Chuah, Raza Ali, and Yizhou Wang. Retinal vessel segmentation using deep learning: a review. *IEEE Access*, 9:111985–112004, 2021.

[4] Mingfei Cheng, Kaili Zhao, Xuhong Guo, Yajing Xu, and Jun Guo. Joint topology-preserving and feature-refinement network for curvilinear structure segmentation. In *Proceedings of the IEEE/CVF International Conference on Computer Vision*, pages 7147–7156, 2021.

[5] Hongwei Du, Xinyue Zhang, Gang Song, Fangxun Bao, Yunfeng Zhang, Wei Wu, and Peide Liu. Retinal blood vessel segmentation by using the ms-lsdnet network and geometric skeleton reconnection method. *Computers in Biology and Medicine*, 153:106416, 2023.

[6] Idris Dulau, Benoit Recur, Catherine Helmer, Cecile Delcourt, and Marie Beurton-Aimar. Connected-components-based post-processing for retinal vessels deep-learning segmentation. In *2023 IEEE 13th International Conference on Pattern Recognition Systems (ICPRS)*, pages 1–7, 2023.

[7] Zhexin Jiang, Hao Zhang, Yi Wang, and Seok-Bum Ko. Retinal blood vessel segmentation using fully convolutional network with transfer learning. *Computerized Medical Imaging and Graphics*, 68:1–15, 2018.

[8] Vinayak S Joshi, Mona K Garvin, Joseph M Reinhardt, and Michael D Abramoff. Identification and reconnection of interrupted vessels in retinal vessel segmentation. In *2011 IEEE International Symposium on Biomedical Imaging: From Nano to Macro*, pages 1416–1420. IEEE, 2011.

[9] Ali Khandouzi, Ali Ariafar, Zahra Mashayekhpour, Milad Pazira, and Yasser Baleghi. Retinal vessel segmentation, a review of classic and deep methods. *Annals of Biomedical Engineering*, 50(10):1292–1314, 2022.

[10] Fausto Milletarì, Nassir Navab, and Seyed-Ahmad Ahmadi. V-net: Fully convolutional neural networks for volumetric medical image segmentation. *2016 Fourth International Conference on 3D Vision (3DV)*, pages 565–571, 2016.

[11] Lei Mou, Li Chen, Jun Cheng, Zaiwang Gu, Yitian Zhao, and Jiang Liu. Dense dilated network with probability regularized walk for vessel detection. *IEEE transactions on medical imaging*, 39(5):1392–1403, 2019.

[12] Meindert Niemeijer, Bram van Ginneken, and Michael D Abràmoff. A linking framework for pixel classification based retinal vessel segmentation. In *Medical Imaging 2009: Biomedical Applications in Molecular, Structural, and Functional Imaging*, volume 7262, pages 333–340. SPIE, 2009.

[13] Jan Odstrcilík, Radim Kolář, Attila Budai, Joachim Hornegger, Jirí Jan, Jirí Gazárek, Tomas Kubena, Pavel Cernosek, Ondrej Svoboda, and Elli Angelopoulou. Retinal vessel segmentation by improved matched filtering: evaluation on a new high-resolution fundus image database. *IET Image Process.*, 7:373–383, 2013.

[14] Wendeson S Oliveira, Joyce Vitor Teixeira, Tsang Ing Ren, George DC Cavalcanti, and Jan Sijbers. Unsupervised retinal vessel segmentation using combined filters. *PloS one*, 11(2):e0149943, 2016.

[15] José Ignacio Orlando, João Barbosa Breda, Karel van Keer, Matthew B. Blaschko, Pablo Javier Blanco, and Carlos Alberto Bulant. Towards a glaucoma risk index based on simulated hemodynamics from fundus images. In *International Conference on Medical Image Computing and Computer-Assisted Intervention*, 2018.

[16] Olaf Ronneberger, Philipp Fischer, and Thomas Brox. U-net: Convolutional networks for biomedical image segmentation. In *Medical Image Computing and Computer-Assisted Intervention–MICCAI 2015: 18th International Conference, Munich, Germany, October 5-9, 2015, Proceedings, Part III 18*, pages 234–241. Springer, 2015.

[17] Suprosanna Shit, Johannes C Paetzold, Anjany Sekuboyina, Ivan Ezhov, Alexander Unger, Andrey Zhylka, Josien PW Pluim, Ulrich Bauer, and Bjoern H Menze. cldice-a novel topology-preserving loss function for tubular structure segmentation. In *Proceedings of the IEEE/CVF Conference on Computer Vision and Pattern Recognition*, pages 16560–16569, 2021.

[18] Karen Simonyan and Andrew Zisserman. Very deep convolutional networks for large-scale image recognition. *CoRR*, abs/1409.1556, 2014.

[19] Joes Staal, Michael David Abràmoff, Meindert Niemeijer, Max A. Viergever, and Bram van Ginneken. Ridge-based vessel segmentation in color images of the retina. *IEEE Transactions on Medical Imaging*, 23:501–509, 2004.

[20] Sumathi Thangaraj, Vivekanandan Periyasamy, and Ravikanth Balaji. Retinal vessel segmentation using neural network. *IET Image Processing*, 12(5):669–678, 2018.

[21] Xiaohong Wang and Xudong Jiang. Post-processing for retinal vessel detection. In *Tenth International Conference on Digital Image Processing (ICDIP 2018)*, volume 10806, pages 1442–1446. SPIE, 2018.

[22] Xiaohong Wang, Xudong Jiang, and Jianfeng Ren. Blood vessel segmentation from fundus image by a cascade classification framework. *Pattern Recognition*, 88:331–341, 2019.

[23] Christian Wiedemann, Christian Heipke, Helmut Mayer, and Olivier Jamet. Empirical evaluation of automatically extracted road axes. *Empirical evaluation techniques in computer vision*, 12:172–187, 1998.

[24] Yicheng Wu, Yong Xia, Yang Song, Yanning Zhang, and Weidong Cai. Nfn+: A novel network followed network for retinal vessel segmentation. *Neural Networks*, 126:153–162, 2020.

[25] Jingdan Zhang, Yingjie Cui, Wuhan Jiang, and Le Wang. Blood vessel segmentation of retinal images based on neural network. In *Image and Graphics: 8th International Confer-*

ence, ICIG 2015, Tianjin, China, August 13-16, 2015, Proceedings, Part II 8, pages 11–17. Springer, 2015.

[26] Shulin Zhang, Rui Zheng, Yuhao Luo, Xuewei Wang, Jianbo Mao, Cynthia J. Roberts, and Mingzhai Sun. Simultaneous arteriole and venule segmentation of dual-modal fundus images using a multi-task cascade network. *IEEE Access*, 7:57561–57573, 2019.